Metabolic Engineering 29 (2015) 217–226

Contents lists available at ScienceDirect

Metabolic Engineering

journal homepage: www.elsevier.com/locate/ymben

Regulating malonyl-CoA metabolism via synthetic antisense RNAs for enhanced biosynthesis of natural products

Yaping Yang [a,1], Yuheng Lin [a,1], Lingyun Li [b], Robert J. Linhardt [b], Yajun Yan [c,*]

[a] College of Engineering, University of Georgia, Athens, GA 30602, USA
[b] Department of Chemistry and Chemical Biology, Center for Biotechnology and Interdisciplinary Studies, Rensselaer Polytechnic Institute, Troy, NY 12180, USA
[c] BioChemical Engineering Program, College of Engineering, University of Georgia, Athens, GA 30602, USA

ARTICLE INFO

Article history:
Received 25 November 2014
Received in revised form
18 March 2015
Accepted 31 March 2015
Available online 9 April 2015

Keywords:
Antisense RNA
Malonyl-CoA
Fatty acid biosynthesis
4-hydroxycoumarin
Resveratrol
Naringenin

ABSTRACT

Malonyl-CoA is the building block for fatty acid biosynthesis and also a precursor to various pharmaceutically and industrially valuable molecules, such as polyketides and biopolymers. However, intracellular malonyl-CoA is usually maintained at low levels, which poses great challenges to efficient microbial production of malonyl-CoA derived molecules. Inactivation of the malonyl-CoA consumption pathway to increase its intracellular availability is not applicable, since it is usually lethal to microorganisms. In this work, we employ synthetic antisense RNAs (asRNAs) to conditionally down-regulate fatty acid biosynthesis and achieve malonyl-CoA enrichment in *Escherichia coli*. The optimized asRNA constructs with a loop-stem structure exhibit high interference efficiency up to 80%, leading to a 4.5-fold increase in intracellular malonyl-CoA concentration when *fabD* gene expression is inhibited. Strikingly, this strategy allows the improved production of natural products 4-hydroxycoumarin, resveratrol, and naringenin by 2.53-, 1.70-, and 1.53-fold in *E. coli*, respectively. In addition, down-regulation of other *fab* genes including *fabH*, *fabB*, and *fabF* also leads to remarkable increases in 4-hydroxycoumarin production. This study demonstrates a novel strategy to enhance intracellular malonyl-CoA and indicates the effectiveness of asRNA as a powerful tool for use in metabolic engineering.

© 2015 International Metabolic Engineering Society. Published by Elsevier Inc. All rights reserved.

1. Introduction

Malonyl-CoA is a universal building block not only for fatty acid biosynthesis, but also for the formation of a variety of natural products, such as coumarins, stilbenes, flavonoids and tetracyclines (Fowler et al., 2009), which have been broadly used as pharmaceuticals and nutraceuticals with various health promoting effects. These compounds are usually generated as secondary metabolites in plants or microorganisms by polyketide synthases (PKSs) through the repeated condensation of various numbers of malonyl-CoA(s) to different starter molecules (Griffin et al., 2010; Han et al., 2011; Leonard et al., 2008; Olano et al., 2011; Yan et al., 2008). For example, 4-hydroxycoumarin, a direct precursor to the widely used anticoagulant warfarin, can be biosynthesized through the condensation of one molecule of malonyl-CoA with salicoyl-CoA; while the formation of naringenin (the gateway molecule to flavonoids) and resveratrol (a representative of stilbene polyphenols) involves the condensation of three malonyl-CoA molecules with *p*-coumaroyl-CoA (Griffin et al., 2010; Han et al., 2011; Lin et al., 2013; Olano et al., 2011). Additionally, tetracyclines and doxorubicin, type II polyketides functioning as potent antibiotics and anti-cancer drugs, require eight and nine malonyl-CoA units for their biosynthesis, respectively (Griffin et al., 2010; Han et al., 2011).

Due to the intrinsic disadvantages associated with their natural producers, such as low productivity, low growth rate, high cultivation cost, and lack of facile genetic tools, growing attention has been placed on developing heterologous microbial cell factories towards economically viable production of these compounds. So far, *Escherichia coli* is still the most preferred host microorganism because of its favorable fermentation properties and ease of genetic manipulation (Xu et al., 2013). In fact, many malonyl-CoA derived natural products have been successfully produced by metabolically engineered *E. coli*, such as 4-hydroxycoumarin, resveratrol, naringenin, phloroglucinol, 7-*O*-methyl aromadendrin, genistein, and daidzein (Griffin et al., 2010; Han et al., 2011; Koirala et al., 2014; Malla et al., 2012; Olano et al., 2011; Zha et al., 2009). In addition, a malonyl-CoA dependent pathway has been constructed for the production of 3-hydroxyproionic acid, an industrially valuable molecule ranked among top of the platform chemicals derived from biomass (Rathnasingh et al., 2012).

However, intracellular malonyl-CoA concentration is usually tightly regulated and maintained at very low levels, which poses

* Correspondence to: 601B Driftmier Engineering Center, University of Georgia, Athens, GA 30602, USA. fax: +1 706 542 8806.
E-mail address: yajunyan@uga.edu (Y. Yan).
[1] These authors have contributed equally to this work.

http://dx.doi.org/10.1016/j.ymben.2015.03.018
1096-7176/© 2015 International Metabolic Engineering Society. Published by Elsevier Inc. All rights reserved.

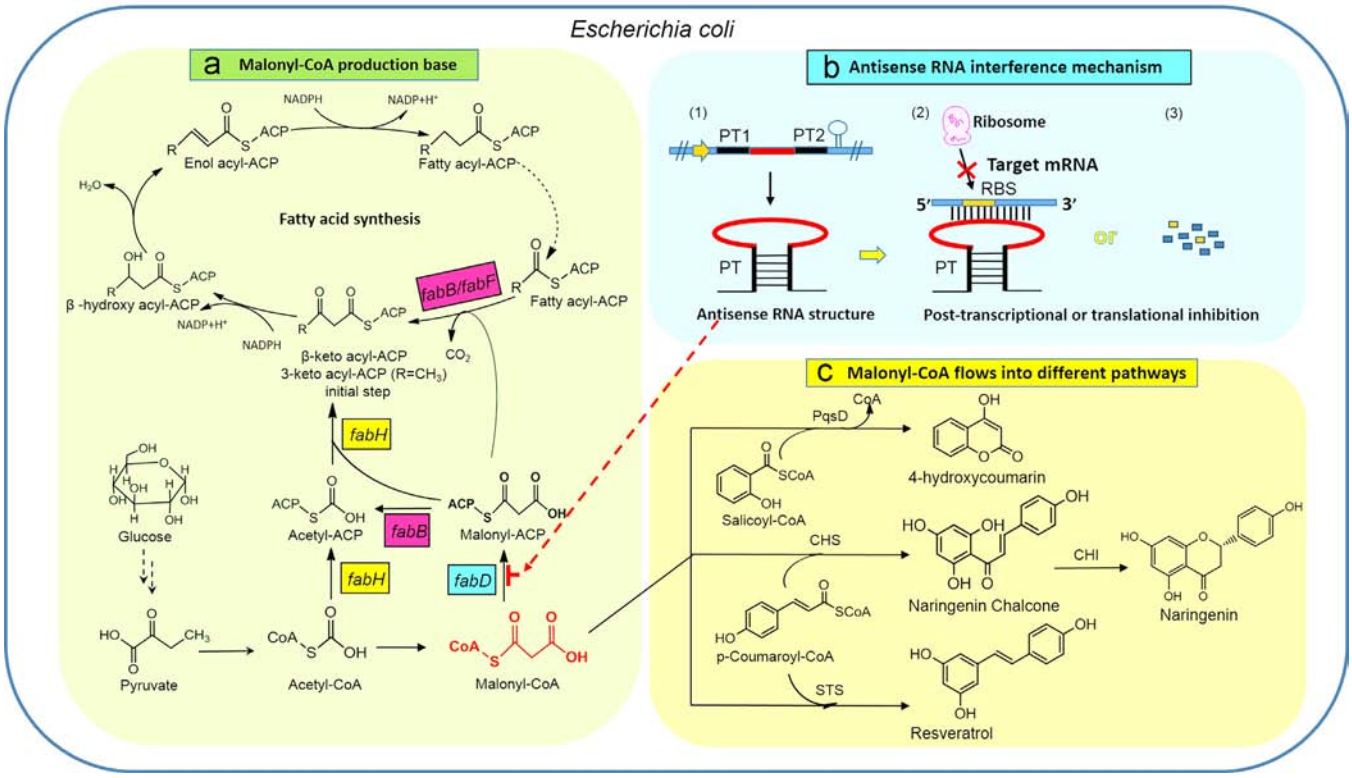

Fig. 1. Engineering of *E. coli* malonyl-CoA metabolic pathways. (a) Malonyl-CoA metabolic networks. *fabD*, encoding malonyl-CoA: ACP transacylase; *fabH*, encoding β-ketoacyl-ACP synthase III; *fabB*, encoding β-ketoacyl-ACP synthase I; *fabF*, encoding β-ketoacyl-ACP synthase II. (b) asRNA interference mechanism. (1) Generation of mature asRNA from DNA. (2) Binding of asRNA to its target mRNA. (3) Degradation of target mRNA. (c) malonyl-CoA fluxes into different polyketide pathways.

great limitation in the productivity of malonyl-CoA derived molecules (Janssen and Steinbuchel, 2014). Therefore, enrichment of intracellular malonyl-CoA pool is of paramount importance for their efficient production. In *E. coli*, malonyl-CoA level is directly determined by the balance of the upstream biosynthesis pathway and the downstream consumption pathway towards fatty acid biosynthesis (Fig. 1a). The previous efforts to improve malonyl-CoA availability were mainly focused on engineering the upstream pathway, such as over-expression of acetyl-CoA carboxylase (ACC) to increase the conversion of acetyl-CoA into malonyl-CoA (Lussier et al., 2012; Xu et al., 2014a), over-expression of acetyl-CoA synthase to enhance acetyl-CoA supply, and deleting acetyl-CoA consumption pathways involved in ethanol and acetate production (Causey et al., 2004). In contrast, few efforts have been made in engineering the malonyl-CoA consumption pathway, since inactivation of fatty acid biosynthesis through conventional gene knockout strategies is usually lethal to host cells (Cronan and Thomas, 2009). Only limited attempts have been reported to use certain antibiotics to inhibit fatty acid biosynthesis. For example, cerulenin, a specific inhibitor to the β-ketoacyl-acyl carrier protein synthases (KAS) I and II (FabB and FabF) (Davis et al., 2000), has been employed to improve the production of polyketides (Leonard et al., 2008; Santos et al., 2011; Xu et al., 2013). However, the use of such antibiotics is usually very costly and, thus, infeasible for application in large-scale production. Here we develop a powerful and inexpensive strategy using antisense RNAs instead of antibiotics to conditionally inhibit fatty acid biosynthesis and reduce undesired malonyl-CoA consumption to overcome this limitation.

Antisense RNAs (asRNAs) are single-stranded RNAs that can complementarily pair with their target mRNA and inhibit gene expression (Nakashima et al., 2006). In plants and yeast, they have been exploited and they exhibit bright prospects as an essential tool to make up the shortcomings of conventional gene knockout strategies (Henz et al., 2007; Scalcinati et al., 2012). However, in bacteria, even though small regulatory RNAs (srRNAs) have been reported, the application of naturally existing asRNAs on the regulation of gene expression has been limited (Storz et al., 2011; Thomason and Storz, 2010). Most reports focus on the design of artificial, synthetic asRNAs and their use in identifying functional genes (Wang and Kuramitsu, 2005), verifying antibacterial mechanisms (Ji et al., 2004), changing antibiotic susceptibility (Sharma et al., 2013), examining rate-limiting genes (Tummala et al., 2003), and regulating gene expression as a riboswitch (Mellin et al., 2013). Despite these exciting achievements, only a few studies have been reported on the metabolic engineering application of asRNAs. Lee's group successfully screened and utilized asRNAs to target 130 library genes, and dramatically improved tyrosine and cadaverine production. Based on the effectiveness of the Hfq scaffold protein, this asRNA structure was expected to be exploited as a tool to modulate gene expression in *E. coli* (Na et al., 2013; Yoo et al., 2013). Prather's group reported the engineering of asRNAs as a metabolite valve to dynamically control central carbon (Solomon et al., 2012). Another study investigated the use of asRNA (RyhB) to improve succinate production in *E. coli* (Kang et al., 2012).

In this work, we further explore and expand the application of asRNAs to target the genes and pathways that are essential for cell viability. We employ an artificial loop-stem scaffold carrying asRNAs and develop them as a tool for down-regulating genes involved in fatty acid biosynthesis. Optimization of asRNA binding lengths results in high interference efficiency (up to 80% inhibition of target gene expression). The engineered *E. coli* strain with *fabD* interfered by its asRNA *asfabD* (100) shows a 4.5-fold increase in intracellular malonyl-CoA concentration. On this basis, the biosynthetic pathways of 4-hydroxycoumarin, resveratrol, and naringenin are introduced into the *fabD*-interfered strain, which leads to significant improvement in their production. In addition, other critical genes involved in fatty acid biosynthesis *fabH*, *fabF*, *fabB* are also targeted with their respective asRNAs, leading to the enhanced production of malonyl-CoA derived 4-hydroxycoumarin as well. This work demonstrates an

effective strategy to enhance malonyl-CoA availability and suggests the great potential of asRNAs for metabolic engineering use, especially for down-regulating the expression of those genes that are essential for cell viability.

2. Materials and methods

2.1. Experimental materials

Luria-Bertani (LB) medium was used to grow *E. coli* cells for plasmid construction, propagation and inoculum preparation. The biosynthesis medium M9Y contains (per liter): glycerol (20 g), yeast extract (5 g), NH_4Cl (1 g), Na_2HPO_4 (6 g), KH_2PO_4 (3 g), NaCl (0.5 g), $MgSO_4 \cdot 7H_2O$ (2 mmol), $CaCl_2 \cdot 2H_2O$ (0.1 mmol) and vitamin B1 (1.0 mg). Ampicillin (100 mg/L), kanamycin (50 mg/L), and/or chloramphenicol (34 mg/L) were added to cultures when necessary. *E. coli* strain XL1-Blue was used for plasmid propagation and gene cloning; BW25113 was used as the host strain for the biosynthesis of 4-hydroxycoumarin, resveratrol and naringenin. Plasmids pZE12-luc, pCS27 and pSA74 are high, medium, and low-copy number plasmids employed for gene cloning, protein expression and pathway assembly in this work (Huo et al., 2011; Lutz and Bujard, 1997; Shen and Liao, 2008). Table 1 lists the strains and plasmids used in this study.

eGFP cDNA (GenBank accession number U55762) was a kind gift from Dr. Gang Cheng group at the Chemical and Biomolecular Engineering Department of University of Akron (OH). The cDNAs of 4CL2 from *Petroselinum crispum*, STS from *Vitis vinifera*, CHI from *Medicago sativa* and CHS from *Petunia hybrida* were generous gifts from Dr. Koffas group at Rensselaer Polytechnic Institute (NY) (Leonard et al., 2006a, 2006b; Lim et al., 2011; Yan et al., 2005a, 2005b).

Phusion High-Fidelity DNA polymerase, DNase I, restriction endonucleases, Quick Ligation Kit and Protoscript II first strand cDNA synthesis kit were purchased from New England Biolabs (Beverly, MA, USA). Zyppy™ Plasmid Miniprep Kit, Zymoclean™ Gel DNA Recovery Kit, and DNA Clean & Concentrator™-5 were purchased from Zymo Research (Irvine, CA, USA). PureLink RNA Mini Kit was purchased from Invitrogen (Carlsbad, CA, USA). FastStart Universal SYBR Green Master (ROX) was purchased from Roche (Basel, Switzerland). Malonyl-CoA, [$^{13}C_3$] -malonyl-CoA and *p*-coumaric acid, were purchased from Sigma (St. Louis, MO, USA). 4-Hydroxycoumarin was purchased from ACROS ORGANICS (Bridgewater, NJ, USA). Resveratrol was purchased from Tokyo Chemical Industry (Portland, OR, USA). Naringenin was purchased from MP Biomedicals (Santa Ana, CA, USA).

2.2. Construction of plasmids

For the eGFP assays, to generate eGFP expression plasmids, the e*gfp* gene was PCR-amplified and subcloned into pZE12-luc between Acc651 and XbaI, yielding pZE-eGFP. Likewise, the amplified e*gfp* gene was subcloned into pCS27 and pSA74 between Acc651 and SalI, resulting pCS-eGFP and pSA-eGFP, respectively. The *fabD* gene with its native RBS was PCR-amplified from *E. coli* MG1655 genomic DNA to produce the DNA sequence of *rfabD*. The DNA sequence of the fusion protein FabD/eGFP with *fabD*'s native RBS was generated by SOE-PCR and cloned into pCS27 and pSA74 using BsiWI and BamHI, yielding pCS-RfabD/eGFP and pSA-RfabD/eGFP, respectively. We constructed

Table 1
Strains and plasmids used in this study.

Strain	Genotype	Source
XL1-blue	*recA*1 *endA*1 *gyrA*96 *thi*-1 *hsdR*17 *supE*44 *relA*1 *lac* [*F′ proAB lacI*^{q}*Z*Δ*M*15 *Tn*10 (*Tet*^{r})]	Stratagene
BW25113	*rrnBT*14 Δ*lacZWJ*16 *hsdR*514 Δ*araBADAH*33 Δ*rhaBADLD*78	CGSC
Plasmids	Description	Reference
pZE12-luc	$P_L$lacO1, *colE* ori, Amp^r	Lutz and Bujard (1997)
pCS27	$P_L$lacO1, *P*15*A* ori, Kan^r	Shen and Liao (2008)
pSA74	$P_L$lacO1, *pSC*101 ori, Cm^r	Huo et al.(2011)
pZE-eGFP	pZE12-luc harboring *egfp*	This study
pCS-eGFP	pCS27 harboring *egfp*	This study
pSA-eGFP	pSA74 harboring *egfp*	This study
pZE-PT	pZE12-luc harboring PT template	This study
pSA-PT	pSA74 harboring PT template	This study
pZE-aseGFP(100)	pZE-PT harboring 100 bp aseGFP DNA	This study
pZE-aseGFP(150)	pZE-PT harboring 150 bp aseGFP DNA	This study
pZE-aseGFP(200)	pZE-PT harboring 200 bp aseGFP DNA	This study
pZE-aseGFP(300)	pZE-PT harboring 300 bp aseGFP DNA	This study
pSA-aseGFP(100)	pSA-PT harboring 100 bp aseGFP DNA	This study
pSA-aseGFP(150)	pSA-PT harboring 150 bp aseGFP DNA	This study
pSA-aseGFP(200)	pSA-PT harboring 200 bp aseGFP DNA	This study
pSA-aseGFP(300)	pSA-PT harboring 300 bp aseGFP DNA	This study
pCS-RfabD/eGFP	pCS27 harboring *fabD* with its native RBS fused with *egfp*	This study
pSA-RfabD/eGFP	pSA74 harboring *fabD* with its native RBS fused with *egfp*	This study
pZE-asfabD(100)	pZE-PT harboring 100 bp as*fabD* DNA	This study
pZE-asfabD(150)	pZE-PT harboring 150 bp as*fabD* DNA	This study
pCS-EPPS	pCS27 harboring *entC, pchB, pqsD* and *sdgA* in one operon	This study
pCS-4CL	pCS27 harboring 4CL2 from *P. crispum*	This study
pCS-STS-4CL	pCS27 harboring STS from *V. vinifera* and 4CL2 from *P. crispum* in one operon	This study
pCS-CHI-CHS	pCS27 harboring CHI from *M. sativa* and CHS from *P. hybrida* in one operon,	This study
pCS-CHI-CHS-4CL	pCS27 harboring CHI from *M. sativa* and CHS from *P. hybrida* in one operon, and 4CL2 from *P. crispum* in the other operon	This study
pZE-asfabH(100)	pZE-PT harboring 100 bp as*fabH* DNA	This study
pZE-asfabH(150)	pZE-PT harboring 150 bp as*fabH* DNA	This study
pZE-asfabB(100)	pZE-PT harboring 100 bp as*fabB* DNA	This study
pZE-asfabB(150)	pZE-PT harboring 150 bp as*fabB* DNA	This study
pZE-asfabF(100)	pZE-PT harboring 100 bp as*fabF* DNA	This study
pZE-asfabF(150)	pZE-PT harboring 150 bp as*fabF* DNA	This study
pZE-asfabD(100)-asfabH(100)	pZE-PT harboring 100 bp as*fabD* DNA and 100 bp *asfabH* with two operons	This study

a parent plasmid pZE-PT. The PT template consists of two inverted repeat DNA sequences (38 bp) termed PT1 and PT2 with a random DNA sequence between them (Nakashima et al., 2006) to facilitate the construction of the plasmids used to produce asRNAs. The random DNA sequence contains two designed restriction sites Acc651 and BamHI to facilitate the insertion of different DNA sequences of asRNAs. The PT template was cloned into the above two plasmids using ApoI and XbaI, yielding pZE-PT and pSA-PT, respectively, to introduce the whole PT template into pZE12-luc and pSA74. The 100, 150, 200 and 300 bp DNA sequences of *egfp* asRNAs were cloned into pZE-PT using Acc651 and BamHI, resulting pZE-aseGFP(100), pZE-aseGFP(150), pZE-aseGFP(200) and pZE-aseGFP(300), respectively, to generate *egfp* asRNA synthesis plasmids. Similarly, plasmids pSA-aseGFP(100), pSA-aseGFP(150), pSA-aseGFP(200) and pSA-aseGFP (300) were generated by using the same cloning strategy. The 100 and 150 bp DNA fragments of *fabD* asRNAs were cloned into pZE-PT using Acc651 and BamHI, resulting pZE-asfabD(100), pZE-asfabD (150), respectively, to generate the *fabD* asRNA synthesis plasmids. Similarly, plasmids pZE-asfabH(100), pZE-asfabH(150), pZE-asfabB (100), pZE-asfabB(150), pZE-asfabF(100) and pZE-asfabF(150) were generated by using the same cloning strategy. The asfabH(100) operon was similarly subcloned into pZE-asfabD(100) using SpeI and SacI, yielding pZE-asfabD(100)-asfabH(100).

For 4-hydroxycoumarin biosynthesis, the DNA fragments *entC-pchB* and *pqsD-sdgA* were amplified from our previous constructed plasmids pZE-EntC-PchB and pCS-PqsD-SdgA (Lin et al., 2013). Then the amplified DNA fragments were subcloned into pCS27 to form one operon through three-piece ligation using Acc651, NdeI and XbaI, yielding plasmid pCS-EPPS. For resveratrol biosynthesis, the genes of 4CL2 and STS were cloned into plasmid pCS27 as one operon using Acc651, BglII, and BamHI, generating pCS-STS-4CL. For naringenin biosynthesis, the gene of 4CL2 was cloned into pCS27 using BglII and Acc651, resulting pCS-4CL. Similarly, the genes of CHI and CHS were cloned as one operon into pCS27 using restriction sites NdeI and BsiWI, yielding pCS-CHI-CHS. The *chi-chs* operon was then subcloned into pCS-4CL using SacI and SpeI, generating pCS-CHI-CHS-4CL.

2.3. Fluorescence assay

The analysis of interference efficiency was performed by measuring the fluorescence intensity using BioTek micro-plate reader. The transformants of *E. coli* BW25113 containing e*gfp* asRNA synthesis plasmids and eGFP expression plasmids and the transformants containing *fadD* asRNA synthesis plasmids and RFabD-eGFP expression plasmids were cultured in 3.5 ml LB medium with appropriate antibiotics at 37 °C and 290 rpm for 5 h. Then 2% cultures were transferred into baffled flasks containing 15 ml of M9Y media with 1 mM IPTG at 30 °C and 290 rpm. At 6 h, 12 h and 18 h, 1 ml aliquots of cell culture were taken and centrifuged at 10,000 rpm, 4 °C for 1 min. The cell pellets were re-suspended in 1 ml of deionized water. Cell cultures (200 μl) were transferred into a black 96-well plate (BRAND plates) and analyzed for eGFP fluorescence intensity using excitation filter of 520 nm, and emission filter of 485 nm. The eGFP fluorescence intensity of each sample was normalized against its OD_{600} and background cell fluorescence was subtracted. Mean values for each sample was obtained from three independent measurements. The reading type was set as endpoint mode (Rapp et al., 2004).

2.4. Quantitative real-time PCR Analysis

All the transformants of *E. coli* BW25113 containing pZE-PT or pZE-asfabD(100) were cultured in 3.5 ml LB medium with appropriate antibiotics at 37 °C and 290 rpm for 5 h. Then 2% cultures were transferred into baffled flasks containing 15 ml of M9Y media with 1 mM IPTG at 30 °C and 290 rpm. After 12 h, 500 μl cell cultures were taken and centrifuged at 10,000 rpm and 4 °C for 1 min. The total RNAs were isolated from the above cell pellets using the PureLink RNA Mini Kit. In this process, all the total RNA samples were treated with DNase I to remove the genomic DNA completely. cDNAs were synthesized from 600 ng of heat-denatured total RNAs using Protoscript II first strand cDNA synthesis kit. qRT-PCR with 12 ng cDNAs was performed using the iQTM SYBR Green Supermix (Bio-Rad) and FastStart Universal SYBR Green Master in 20 μl reaction volume (at least in triplicate) under the following cycling conditions: 95 °C for 30 s; 95 °C for 10 min; followed by 45 cycles of 95 °C for 15 s; 58 °C for 30 s; 72 °C for 20 s. As a normalizer gene, 16sRNA was amplified with primers (F-5'-GCTCGTGTTGTGAAATGTT, R-5'-TGTAGCCCTGGTCGTAAGG) and the product size was 150 bp. The *fabD* gene fragment was amplified with primers (F-5'-TGAAGAACTGAATAAAACC, R-5'-GCAATAGACG-CATCATCCA) and the product size was 274 bp. The specificity of *fabD* primers was confirmed using a BLAST analysis against the NCBI genome database. The integrities of the obtained products were verified by gel electrophoresis on 2% agarose (in 1 × TAE buffer) gels. In addition, a melting curve analysis was carried out for each reaction under the following condition: 55 °C to 95 °C; 0.5 °C/read; 1 s hold; 72 °C for 10 min. The relative quantification of gene expression between the *E. coli* BW25113 containing plasmid pZE-asfabD(100) and the strain containing plasmid pZE-PT was calculated by the $2^{-\Delta\Delta Ct}$ approximation method (Livak and Schmittgen, 2001).

2.5. Extraction of intracellular malonyl-CoA

All the transformants of *E. coli* BW25113 containing pZE-PT or pZE-asfabD(100) were cultured in 3.5 ml LB medium with appropriate antibiotics at 37 °C and 290 rpm for 5 h. Then 2% cultures were transferred into baffled flasks containing 50 ml of M9Y media with 1 mM IPTG at 30 °C and 290 rpm. After 6 h and 12 h, 20.5 ml and 10.5 ml cell cultures were taken and chilled on ice, respectively. Then the cultures were centrifuged at 6000 rpm and 4 °C for 8 min. The supernatants were discarded and the cell pellets were individually re-suspended in 1 ml of 6% perchloric acid (0.125 ml/mg cell) to facilitate cell lysis. Each of the lysed cell suspension was then neutralized with 3 M potassium carbonate (0.3 ml/ml cell lysate). Additionally, 700 ng/ml of [$^{13}C_3$]-malonyl-CoA was spiked into the above mixtures as internal standard and centrifuged at 6000 rpm and 4 °C for 8 min. Then, 1.5 ml of supernatant was loaded into a solid-phase extraction column (Sep-Pak C18 Plus Short Cartridge, Waters, WAT020515) pre-conditioned with 2 ml methanol and 2 ml formic acid (pH 3.0), respectively (Minkler et al., 2006; Xu et al., 2014b). The loaded column was then washed with 2 ml water and eluted with 1 ml methanol. The eluted samples were dried under a nitrogen stream at 4 °C and dissolved with 150 μl of 0.1% formic acid in 10 mM ammonium acetate/methanol (80:20) for LC/MS/MS (Onorato et al., 2010). Dry cell weight was calculated according to the empirical rule that 1 OD_{600} = 0.36 g/L (Patnaik et al., 1992).

2.6. LC-MS/MS analysis of malonyl-CoA

Sample analysis was performed with a LC-MS/MS system using an Agilent 1200 (Agilent Technologies, Santa Clara, CA, USA) separation module connected directly to a Thermo TSQ Ultra triple quadrupole MS system (Thermo Fisher Scientific, San Jose, CA. USA). A 100 × 2.1 mm C18 reverse-phase HPLC column (Thermo Fisher Scientific, San Jose, CA. USA) was used to perform HPLC separation. The analytes were eluted at a flow rate of 250 μl/min with a gradient of 25 mM ammonium acetate (mobile phase A) and 25 mM ammonium acetate in 90% acetonitrile (mobile phase B). Agilent 1200 HPLC binary

pump was used to deliver the gradient from 2% to 20% B over 15 min at a flow rate of 250 μl/min after injecting the samples. The column effluent was directed to Thermo TSQ MS instrument working on ESI positive mode with SRM (selected ion monitor) setting. The instrument was tuned and SRM conditions were optimized by the direct infusion of a solution of standard malonyl-CoA (100 μM) in the ESI ion source with the same mobile phase used for HPLC separation. The transitions (m/z parent→m/z daughter) for the malonyl-CoA were as follows: (1) malonyl-CoA, 854→347; (2) [$^{13}C_3$]-malonyl-CoA, 857→350. The ratio of measured peak area of malonyl-CoA to the peak area of internal standard ([$^{13}C_3$]-malonyl-CoA) was used for relative quantification.

2.7. HPLC-quantitative analysis

Both the standards and samples were quantitatively analyzed by HPLC (Dionex Ultimate 3000) with a reverse-phase ZORBAX SB-C18 column and an Ultimate 3000 Photodiode Array Detector. All the transformants used for the biosynthesis of 4-hydroxycoumarin, resveratrol and naringenin were cultured in 3.5 ml LB medium with appropriate antibiotics at 37 °C and 290 rpm for 5 h, then 2% cultures were transferred into baffled flasks containing 15 ml M9Y media with 1 mM IPTG (for resveratrol and naringenin biosynthesis, 1 mM *p*-coumaric acid were added) at 30 °C and 290 rpm. After 24 h, 1 ml cultures were taken to measure OD_{600} values and analyze the products by HPLC.

For the 4-hydroxycoumarin HPLC analysis, solvent A was 0.1% (vol/vol) formic acid in water and solvent B was 100% methanol. The gradient was at a flow rate of 1 ml/min: 20–80% solvent B for 18 min, 80–20% solvent B for 1 min and 20% solvent B for additional 4 min. The 4-hydroxycoumarin peak eluted at 11.69 min with this program. For resveratrol and naringenin analysis, solvent A was 0.1% (vol/vol) formic acid in water and solvent B was 100% acetonitrile. The gradient was 30% solvent B for 15 min at a flow rate of 1 ml/min. The resveratrol and naringenin peaks appeared at 4.25 and 8.89 min, respectively. Quantification was based on the peak area in reference to the commercial standards. 4-Hydroxycoumarin and naringenin were detected and quantified by monitoring absorbance at 285 nm. The resveratrol was detected and quantified by monitoring absorbance at 310 nm. Samples containing over 100 mg/L of products were diluted before running HPLC to maintain a linear concentration–peak area relationship.

3. Results

3.1. Development of asRNA tool and characterization of its properties

Sufficient and controllable interference efficiency is a prerequisite for the application of asRNAs in genetic manipulation. Among all the factors that may affect interference efficiency, asRNA stability was primarily taken into consideration. Previous studies have shown that improvement in asRNA stability can lead to enhanced interference efficiency. It has been reported that the stem-loop structure can significantly enhance its stability and increase the asRNA lifetime (Nakashima et al., 2006). In this work, we employed this structure as a scaffold to develop the asRNA tool. We constructed a plasmid carrying two inverted repeat sequences and then inserted the DNA fragment corresponding to the asRNA between them to generate this stem-loop structure. When transcribed into RNA in *E. coli*, the two inverted repeats would complementarily pair with each other and form a double-strand stem structure termed as paired termini (PT); meanwhile the interposed RNA sequence would form the loop (Fig. 1b). We employed the enhanced green fluorescence protein (eGFP) as a reporter to test the interference efficiency of the above asRNA structure. When the asRNA loop complementarily pairs with the eGFP mRNA, the resulting steric effect would inhibit the binding of ribosome and decrease the translation of eGFP (Fig. 1b).

The translation initiation region on mRNA covering the ribosome binding site (RBS) and start codon has been reported to be an ideal target for asRNA-mediated gene silencing (Crosby et al., 2012; Nakashima et al., 2006). In this work, we still selected this target region but further studied the effect of asRNA loop length on interference efficiency. Four asRNAs with various loop lengths (100, 150, 200 and 300 nt) complementary to eGFP mRNA were selected, all of which initiate from the −20 nt upstream the RBS. Initially, we employed a high-copy-number (50–70) plasmid pZE-aseGFP for asRNA generation, and a low-copy-number (10–12) plasmid pSA-eGFP for the reporter eGFP expression. When the two plasmids were co-transferred into *E. coli*, the asRNAs with different lengths exhibited varied interference efficiencies. The construct with a 100-nt loop decreased the eGFP fluorescence intensity by about 80% during 6–24 h, compared with the RNA scaffold without the loop; while the interference efficiencies of the asRNAs with 150-, 200- and 300-nt loops were 44%, 50% and 38% on average, respectively (Fig. 2). These results suggested that longer asRNA sequences do not necessarily lead to higher interference efficiencies. In addition, we observed that the interference efficiencies at 3 h were slightly higher than those after 6 h for all loop lengths.

Furthermore, we also examined the effect of the relative abundance between asRNAs and their target mRNAs on the interference efficiencies. When we continued using the high-copy-number plasmid for asRNA generation, but employed a medium-copy-number (20–30) plasmid pCS-eGFP instead of the low-copy-number plasmid to express the reporter eGFP, the interference efficiency of the 100-nt asRNA decreased from 80% to 65%; while no significant change in interference efficiency was observed for other lengths. Interestingly, when we used a low-copy-number plasmid (10–12) pSA-aseGFP for asRNA synthesis but a high-copy-number plasmid for eGFP expression, the interference efficiencies for all the asRNAs fell below 20%. These results indicated that high abundance of asRNAs relative to their target mRNAs is critical to achieve high interference efficiency. It is also reasonable to conclude that asRNAs generated with high-copy-number plasmids should be more efficient in down-regulating the expression of chromosomal genes.

3.2. Design and characterization of asRNAs targeting fabD

In the fatty acid biosynthesis, several genes, such as *fabD*, *fabF* and *fabB* are involved in malonyl-CoA consumption. Particularly, the malonyl-CoA: ACP transacylase encoded by *fabD* is the first step for malonyl-CoA consumption, leading to the generation of malonyl-ACP. Previous studies have reported that the genetic inactivation of gene *fabD* was lethal for cells (Janssen and Steinbuchel, 2014). In this study, we first targeted this gene to demonstrate the effectiveness of asRNAs on the repression of fatty acid biosynthesis and enrichment of cellular malonyl-CoA. However, to facilitate the measurement of *fabD* interference, we constructed a FabD/eGFP fusion protein, which can indicate the expression level of gene *fabD* through fluorescence signal monitoring. We introduced the native RBS of *fabD* upstream the FabD/eGFP gene and cloned them into a low-copy-number plasmid pSA74, yielding pSA-RfabD/eGFP to better simulate the expression of chromosomal genes. However, the FabD/eGFP fusion protein expressed by this low-copy plasmid showed very weak fluorescence signal, which was inconvenient for measurement due to the sensitivity limit of the detection device. Thus, we shifted to a medium-copy plasmid pCS-RfabD/eGFP for expressing the fusion protein instead of pSA-RfabD/eGFP (Fig. 3a). Meanwhile, we designed *asfabD* targeting the RBS and coding region of *fabD* mRNA and generate it with a high copy number

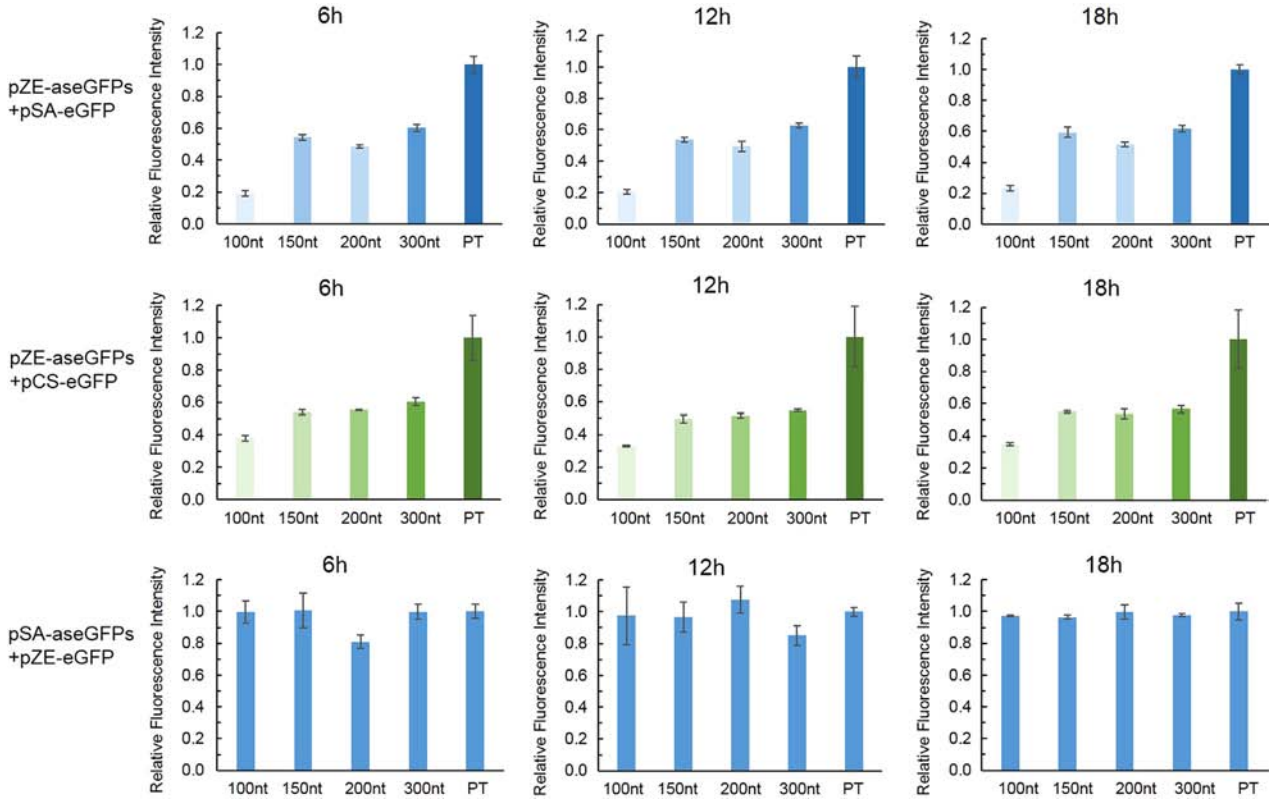

Fig. 2. Interference efficiencies of asRNAs with varied loop lengths and relative abundance. (a) eGFP expression (low copy) interfered by asRNAs (high copy) with 100, 150, 200 and 300-nt loop lengths. (b) eGFP expression (medium copy) interfered by asRNAs (high copy). (c) eGFP expression (high copy) interfered by asRNAs (low copy). We set the relative fluorescence intensity of the negative control strains carrying pZE-PT or pSA-PT as 1.0 (or 100%) for each time point. Interference efficiency (%) = 100% – relative fluorescence intensity. All the data points were normalized by their respective OD_{600} values. The results were generated from three independent experiments.

plasmid pZE-asfabD(100). When pZE-asfabD(100) and pCS-RfabD/eGFP were co-transferred into *E. coli*, the green fluorescence intensity decreased by 58.8% (Fig. 3b) compared with the control strain carrying pZE-PT and pCS-RfabD/eGFP, indicating that the developed asRNA tool is applicable for the *fabD* interference.

3.3. The effect of asfabD interference at transcriptional and metabolite level

Previous studies indicated that asRNA may not only function at the translational level, but also repress gene transcription or trigger mRNA degradation (Shi et al., 2014). We introduced pZE-asfabD(100) into wild-type *E. coli* and performed real-time PCR to detect the variation of the *fabD* mRNA level to verify whether the *fabD* expression was interfered before translation. As shown in Fig. 3c, the relative mRNA levels of gene *fabD* (from five transformants) were remarkably reduced at 12 h, compared with those of the control strain carrying pZE-PT, (from three transformants), indicating that the as*fabD* can cause the decrease of intracellular *fabD* mRNA abundance. We detected malonyl-CoA concentration by LC-MS/MS to further investigate whether the down-regulated expression of gene *fabD* can result in the enrichment of cellular malonyl-CoA. As shown in Fig. 4, the engineered strain carrying pZE-asfabD(100) showed 4.37 and 4.52-fold increases in malonyl-CoA concentration at 6 h and 12 h, respectively, compared with the control strain with pZE-PT. The results above clearly demonstrate that asRNA-mediated down-regulation of *fabD* gene expression occurred at post-transcriptional and translational level, the overall effect of which is the repression of fatty acid biosynthesis and the enrichment of malonyl-CoA.

3.4. Production enhancement of malonyl-CoA derived molecules by asfabD interference

We firstly used the biosynthesis of 4-hydroxycoumarin, a pathway well established in our previous work (Lin et al., 2013), as a demonstration to examine if the enriched malonyl-CoA pool can be redirected into desired pathways. Four pathway genes encoding EntC, PfPchB, PqsD and SdgA were consecutively cloned as an operon in a medium-copy-number plasmid pCS-EPPS (Fig. 5a). When pCS-EPPS and pZE-asfabD(100) were simultaneously introduced into *E. coli* BW25113, the resulting strain produced 270.85 mg/L of 4-hydroxycoumarin at 24 h. In contrast, the control strain BW25113 carrying pCS-EPPS and pZE-PT (a backbone plasmid without asRNA loop) was only able to produce 106.95 mg/L 4-hydroxycoumarin, indicating that inhibition of *fabD* expression by asRNA led to a 2.53-fold increase in the 4-hydroxycoumarin titer (Fig. 5b). In addition, we observed that the *fabD* down-regulated strain did not show obvious growth retardation (Table 2).

Two other established pathways leading to the biosynthesis of model polyketides resveratrol and naringenin were also tested to further verify the effect of the down-regulated *fabD* expression on the production of other malonyl-CoA derived molecules. Previous studies reported that over-expression of 4-coumarate:CoA ligase (4CL) and stilbene synthesis (STS) in *E. coli* led to the production of resveratrol from *p*-coumaric acid; while the production of naringenin requires the expression of 4CL, chalcone synthase (CHS) and chalcone isomerase (CHI) (Leonard et al., 2008; Yan et al., 2008). Therefore, we constructed two plasmids pCS-STS-4CL and pCS-CHI-CHS-4CL to express the genes involved in resveratrol and naringenin biosynthesis, respectively. When these two plasmids were separately co-transferred with the control plasmid pZE-PT

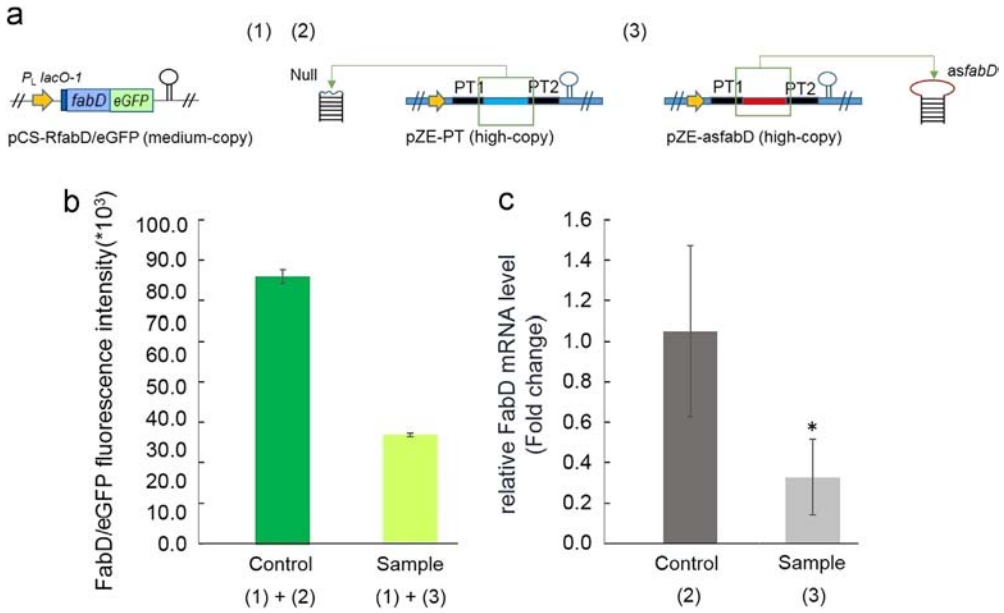

Fig. 3. Effects of the *fabD* asRNA at translational and post-transcriptional levels. (a) Schematic representation of plasmid construction. (1) FabD/eGFP fusion protein expressed by a medium-copy-number plasmid. (2) Negative control plasmid only containing the stem structure (PT sequences) without asRNA loop. (3) asRNA generating plasmid containing the *fabD* asRNA with a 100-nt loop; (b) Fluorescence intensity of FabD/eGFP fusion protein interfered by as*fabD*(100). The results were generated from three independent experiments; (c) Relative mRNA level of gene *fabD* in *E. coli* strains. For the negative controls, three different transformants were used; for the samples, five different transformants were used. For each transformant, qRT-PCR was repeated for three times. For each transcript of gene *fabD* in all samples and negative controls, the values are normalized to the internal control (16srRNA). *: $p=0.04$ was analyzed by unpaired, one-tailed Student's t test.

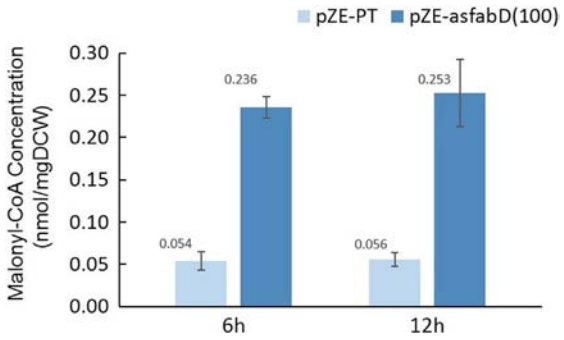

Fig. 4. Intracellular concentrations of malonyl-CoA. Light blue: strain expressing null asRNAs (negative control). Dark blue: the strain expressing *fabD* asRNA with a 100-nt loop. DCW: dry cell weight. The results were generated from three independent experiments. (For interpretation of the references to color in this figure legend, the reader is referred to the web version of this article.)

into *E. coli*, the titers of resveratrol and naringenin achieved 158.22 and 59.58 mg/L, respectively. In contrast, when the pCS-STS-4CL was co-transformed with pZE-asfabD(100), the resveratrol titers achieved 268.20 mg/L, a 1.70-fold increase compared with the control strain (Fig. 5c); while naringenin titer for the strain carrying pCS-CHI-CHS-4CL and pZE-asfabD(100) was 91.31 mg/L, representing a 1.53-fold improvement (Fig. 5d). All the significant titer improvements for these three heterologous products demonstrate that asRNAs have been developed as a powerful tool to inhibit essential genes.

3.5. Effects of other down-regulated fab genes on 4-HC pathway

In addition to *fabD*, we also examined the effect of the down-regulation of other *fab* genes including *fabB* and *fabF* and *fabH* on 4-HC biosynthesis. As shown in the Fig. 1a, β-oxoacyl-ACP synthase I (KAS I) encoded by gene *fabB* catalyze the repeated condensation of malonyl-ACP to form β-oxoacyl-ACP; while KAS II encoded by *fabF* is an isoenzyme of KAS I, which is also responsible for the elongation of fatty acid chains (Lee et al., 2013; Price et al., 2001). Since both of these consume the intermediate downstream of malonyl-CoA, we further selected these two targets for asRNA interference study. Using similar approaches, we constructed two plasmids pZE-asfabB(100) and pZE-asfabF(100) to generate the asRNAs with 100-nt loops targeting *fabB* and *fabF*, respectively. When pZE-asfabB(100) and pZE-asfabF(100) were separately transferred with pCS-EPPS carrying 4-hydroxycoumarin biosynthetic genes into *E. coli*, as shown in Table 2, 4-hydroxycoumarin was produced at the titers of 116.95 and 173.66 mg/L, representing a 1.09-fold and a 1.62-fold increase, respectively, compared with the control strain without asRNA interference (106.95 mg/L, see Section 3.4). Apparently, the repression of *fabB* and *fabF* is not as efficient as that of *fabD*. However, we observed that the *fabB* and *fabF*-interfered strains showed obvious growth retardation compared with the *fabD*-interfered strain during the early stage of cultivation (data not shown). We speculated that the interference efficiency of the asRNAs with 100-nt loops might be excessively high for *fabB* and *fabF* repression, which is harmful to normal cell growth. We employed weaker asRNAs with 150-nt instead of 100-nt lengths to verify this hypothesis. As shown in Table 2, the strains with *fabB* and *fabF* interfered by the asRNAs with 150-nt loops showed a 1.79-fold and a 2.49-fold increase in 4-hydroxycoumarin titers, respectively, much higher than those by the asRNAs with 100-nt loops. In addition, 3-ketoacyl-ACP synthase III encoded by *fabH* was also tested. Employment of the asRNAs with 100 and 150-nt loops led to a 1.86-fold and a 2.12-fold increase in 4-hydroxycoumarin production, respectively, showing a similar trend to *fabB* and *fabF* interference. Based on these results, we conclude that high interference efficiency on the fatty acid biosynthesis is not always beneficial for the production of malonyl-CoA derived compounds. Balanced allocation of malonyl-CoA between cell growth and heterologous molecules production is desirable to prevent the impairment of cell viability.

In addition to targeting single genes, we also explored the simultaneous interference of two genes by asRNAs to investigate whether the effect of malonyl-CoA enrichment can be accumulated. As shown in Table 2, interferences of single genes *fabD* and *fabH* by the asRNAs with 100-nt loops are among the most efficient ones in improving 4-hydroxycoumarin production.

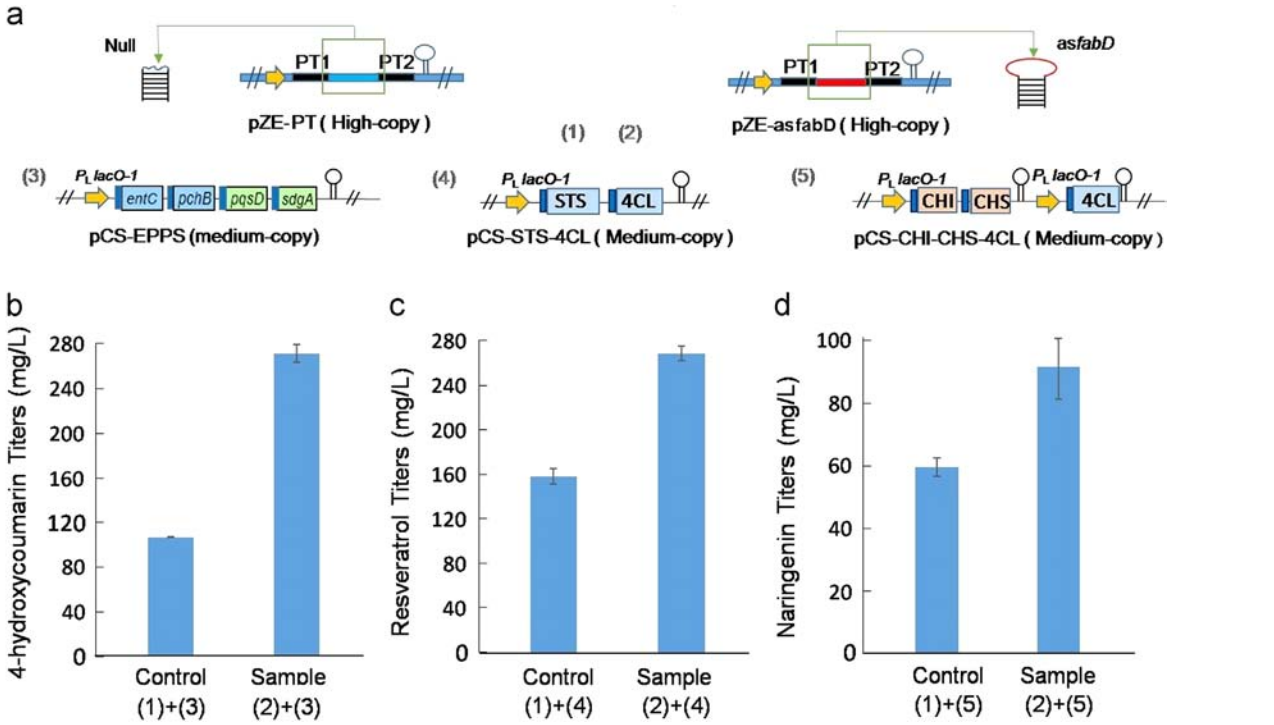

Fig. 5. Heterologous production of malonyl-CoA derived compounds with and without the effects of asRNAs. (a) Schematic representation of plasmid construction. (1) Negative control plasmid. (2) asRNA generating plasmid. (3) The plasmid carrying 4-hydroxycoumarin biosynthetic genes. (4) The plasmid carrying resveratrol biosynthetic genes. (5) The plasmid carrying naringenin biosynthetic genes. (b) 4-hydroxycoumarin titers; (c) resveratrol titers; (d) naringenin titers. The results were generated from three independent experiments.

Table 2
Effect of down-regulated *fab* genes on 4-hydroxycoumarin production.

Negative control	**OD_{600}**	**4-HC Titers(mg/L)**	**Fold**
pZE-PT + pCS-EPPS	9.33 ± 0.11	106.95 ± 0.13	1.00
Loop size = 100 nt	**OD_{600}**	**4-HC Titers(mg/L)**	**Fold**
pZE-asfabH + pCS-EPPS	8.71 ± 0.13	199.43 ± 9.78	1.86
pZE-asfabF + pCS-EPPS	8.01 ± 0.88	173.66 ± 10.86	1.62
pZE-asfabB + pCS-EPPS	8.74 ± 0.29	116.95 ± 15.90	1.09
pZE-asfabD + pCS-EPPS	9.34 ± 0.96	270.85 ± 7.85	2.53
pZE-asfabD-asfabH + pCS-EPPS	8.71 ± 0.13	235.22 ± 7.25	2.20
Loop size = 150 nt	**OD_{600}**	**4-HC Titers(mg/L)**	**Fold**
pZE-asfabH + pCS-EPPS	10.02 ± 0.05	226.23 ± 1.99	2.12
pZE-asfabF + pCS-EPPS	8.63 ± 0.07	266.41 ± 7.00	2.49
pZE-asfabB + pCS-EPPS	8.78 ± 0.29	191.91 ± 20.5	1.79
pZE-asfabD + pCS-EPPS	8.14 ± 0.18	212.34 ± 7.36	1.99

All data are reported as mean ± s.d. from three independent experiments.

Therefore, we constructed a plasmid pZE-asfabD(100)-asfabH(100) to generate the asRNAs with 100-nt loops targeting *fabD* and *fabH* simultaneously. When it was transferred into *E. coli* together with pCS-EPPS, we observed a 2.20-fold increase in 4-hydroxycoumarin production compared with the control strain without asRNA interference, which is slightly lower than the strain with only *fabD* interfered (2.53-fold). These results suggested that *fabD* is the most desired target to inhibit the malonyl-CoA consumption. Additional interference of other *fab* genes may not further improve the titers of malonyl-CoA derived compounds significantly.

4. Discussion

Gene knock-out strategy has been playing a significant role in charactering gene functions or engineering cells for desirable metabolic properties (Nakashima and Tamura, 2009). However, this strategy is usually limited to those genes that are not essential for cell growth. Alternatively, asRNA has been exploited to overcome this limitation by conditionally down-regulating the expression of essential target genes. Through binding to the translation initiation region (e.g. RBS and start codon) of target mRNA, a reversible steric effect leads to a knockdown regulation by blocking the ribosome reading through mRNA and inhibiting the translation of the corresponding genes (Nakashima and Tamura, 2009). This property promoted us to investigate the factors critical for interference efficiency and strategies to control the efficiency.

In this study, we employed an artificial stem-loop structure to improve the stability of asRNA, then optimized its loop size to achieve the fine-tuning of its interference efficiency. We observed from the results that shorter asRNAs exhibited higher interference efficiency within the range of 100–300 nt. We speculated that the longer loops might form more complicated secondary structures that weaken their binding to target mRNAs or decrease the asRNA stability. Additionally, we observed that higher relative abundance of asRNA over its target gene was critical to achieve high interference efficiency (Fig. 2). Based on the generalized rules, we applied asRNAs to interfere fatty acid biosynthesis genes. We evaluated its interference efficiency and demonstrated its effect at transcriptional, translational and metabolic levels through real-time PCR, eGFP fusion protein reporter and LC/MS/MS, respectively. In practice, the single interference of *fabD* led to a 4.52-fold increase in intracellular malonyl-CoA concentration, demonstrating the effectiveness of the *fabD* asRNA. Then, we introduced the designed *fabD* asRNA into three heterologous pathways of malonyl-CoA derived natural products and achieved 2.53-fold, 1.70-fold and 1.53-fold increases in 4-hydroxycoumarin, resveratrol and naringenin production, respectively. Apparently, the titers of these compounds were not increased as much as the level of malonyl-CoA, which may be explained by the following two reasons. On one hand, the enriched malonyl-CoA might have saturated the heterologous enzymes; on the other hand,

these pathways involve other precursors (e.g. salicoyl-CoA and *p*-coumaroyl-CoA), which may also be determinative factors for production.

We used the biosynthesis of 4-hydroxycoumarin as a model system, and targeted other genes directly and/or indirectly related to malonyl-CoA consumption with asRNAs to further investigate this strategy. As shown in Table 2, in addition to gene *fabD*, interference of other genes such as *fabB, fabF* and *fabH* also led to significant improvements in 4-hydroxycoumarin production. However, the interference efficiency has varied effects on the different *fab* genes. For example, the interference of gene *fabD* with the asRNAs with 100 and 150-nt loops showed similar results; while for *fabB, fabF* and *fabH,* the asRNAs with 150-nt loops were obviously advantageous than the asRNAs with 100-nt loops. Meanwhile, we observed growth retardation for strains with genes *fabB, fabF* and *fabH* interfered by the asRNAs with 100-nt loops, indicating that excessively strong inhibition of these genes may impair cell viability. Based on the analysis above, we conclude that high interference efficiency is not always necessary to achieve high titers. A balanced allocation of malonyl-CoA between necessary cell growth and heterologous production is critical to maintain the desired viability of the microbial cell factories and achieve the most efficient production. Therefore, asRNA design and interference efficiency should be further investigated to provide more controllable tools for metabolic engineering use. As we were preparing this manuscript, the use of antisense RNA strategy to enhance the production of naringenin was reported (Wu et al., 2014). Compared with this work which focused on a single target product, we have demonstrated that regulating malonyl-CoA using antisense RNA can be a platform technology for improving the production of a variety of molecules (e.g. 4-HC, resveratrol and naringenin) derived from malonyl-CoA. In addition, we conducted a more systematic study on the effect of down-regulating several fatty acid biosynthesis genes on the enrichment of intercellular malonyl-CoA. Overall, this work demonstrates that antisense RNA is a promising genetic tool to increase microbial production of economically and pharmaceutically valued compounds.

Conflict of interest

No conflict of interest.

Acknowledgments

This work was supported by the start-up funds from the College of Engineering, University of Georgia, Athens; a portion of a research grant provided by the University of Georgia Research Foundation, Inc.; and a Scientist Development Grant (11SDG6960001) from the American Heart Association. The authors thank Dr. Gang Cheng and Dr. Mattheos Koffas for kindly providing experimental materials.

References

Causey, T.B., Shanmugam, K.T., Yomano, L.P., Ingram, L.O., 2004. Engineering *Escherichia coli* for efficient conversion of glucose to pyruvate. Proc. Natl. Acad. Sci. USA 101, 2235–2240.

Cronan, J.E., Thomas, J., 2009. Bacterial fatty acid synthesis and its relationships with polyketide synthetic pathways. Methods Enzymol. 459, 395–433.

Crosby, H.A., Rank, K.C., Rayment, I., Escalante-Semerena, J.C., 2012. Structure-guided expansion of the substrate range of methylmalonyl coenzyme A synthetase (MatB) of *Rhodopseudomonas palustris*. Appl. Environ. Microbiol. 78, 6619–6629.

Davis, M.S., Solbiati, J., Cronan Jr., J.E., 2000. Overproduction of acetyl-CoA carboxylase activity increases the rate of fatty acid biosynthesis in *Escherichia coli*. J. Biol. Chem. 275, 28593–28598.

Fowler, Z.L., Gikandi, W.W., Koffas, M.A., 2009. Increased malonyl coenzyme A biosynthesis by tuning the *Escherichia coli* metabolic network and its application to flavanone production. Appl. Environ. Microbiol. 75, 5831–5839.

Griffin, M.O., Fricovsky, E., Ceballos, G., Villarreal, F., 2010. Tetracyclines: a pleitropic family of compounds with promising therapeutic properties. Review of the literature. Am. J. Physiol. Cell Physiol. 299, C539–C548.

Han, A.R., Park, J.W., Lee, M.K., Ban, Y.H., Yoo, Y.J., Kim, E.J., Kim, E., Kim, B.G., Sohng, J.K., Yoon, Y.J., 2011. Development of a Streptomyces venezuelae-based combinatorial biosynthetic system for the production of glycosylated derivatives of doxorubicin and its biosynthetic intermediates. Appl. Environ. Microbiol. 77, 4912–4923.

Henz, S.R., Cumbie, J.S., Kasschau, K.D., Lohmann, J.U., Carrington, J.C., Weigel, D., Schmid, M., 2007. Distinct expression patterns of natural antisense transcripts in Arabidopsis. Plant Physiol. 144, 1247–1255.

Huo, Y.X., Cho, K.M., Rivera, J.G.L., Monte, E., Shen, C.R., Yan, Y.J., Liao, J.C., 2011. Conversion of proteins into biofuels by engineering nitrogen flux. Nat. Biotechnol. 29 346–U160.

Janssen, H.J., Steinbuchel, A., 2014. Fatty acid synthesis in *Escherichia coli* and its applications towards the production of fatty acid based biofuels. Biotechnol. Biofuels 7, 7.

Ji, Y., Yin, D., Fox, B., Holmes, D.J., Payne, D., Rosenberg, M., 2004. Validation of antibacterial mechanism of action using regulated antisense RNA expression in *Staphylococcus aureus*. FEMS Microbiol. Lett. 231, 177–184.

Kang, Z., Wang, X., Li, Y., Wang, Q., Qi, Q., 2012. Small RNA RyhB as a potential tool used for metabolic engineering in *Escherichia coli*. Biotechnol. Lett. 34, 527–531.

Koirala, N., Pandey, R.P., Van Thang, D., Jung, H.J., Sohng, J.K., 2014. Glycosylation and subsequent malonylation of isoflavonoids in *E. coli*: strain development, production and insights into future metabolic perspectives. J. Ind. Microbiol. Biotechnol. 41, 1647–1658.

Lee, S., Lee, S., Yoon, Y.J., Lee, J., 2013. Enhancement of long-chain fatty acid production in *Escherichia coli* by coexpressing genes, including *fabF*, involved in the elongation cycle of fatty acid biosynthesis. Appl. Biochem. Biotechnol. 169, 462–476.

Leonard, E., Chemler, J., Lim, K.H., Koffas, M.A., 2006a. Expression of a soluble flavone synthase allows the biosynthesis of phytoestrogen derivatives in *Escherichia coli*. Appl. Microbiol. Biotechnol. 70, 85–91.

Leonard, E., Yan, Y., Fowler, Z.L., Li, Z., Lim, C.G., Lim, K.H., Koffas, M.A., 2008. Strain improvement of recombinant *Escherichia coli* for efficient production of plant flavonoids. Mol. Pharm. 5, 257–265.

Leonard, E., Yan, Y.J., Koffas, M.A.G., 2006b. Functional expression of a P450 flavonoid hydroxylase for the biosynthesis of plant-specific hydroxylated flavonols in *Escherichia coli*. Metab. Eng. 8, 172–181.

Lim, C.G., Fowler, Z.L., Hueller, T., Schaffer, S., Koffas, M.A., 2011. High-yield resveratrol production in engineered *Escherichia coli*. Appl. Environ. Microbiol. 77, 3451–3460.

Lin, Y., Shen, X., Yuan, Q., Yan, Y., 2013. Microbial biosynthesis of the anticoagulant precursor 4-hydroxycoumarin. Nat. Commun. 4, 2603.

Livak, K.J., Schmittgen, T.D., 2001. Analysis of relative gene expression data using real-time quantitative PCR and the 2(-Delta Delta C(T)) method. Methods 25, 402–408.

Lussier, F.X., Colatriano, D., Wiltshire, Z., Page, J.E., Martin, V.J., 2012. Engineering microbes for plant polyketide biosynthesis. Comput. Struct. Biotechnol. J. 3, e201210020.

Lutz, R., Bujard, H., 1997. Independent and tight regulation of transcriptional units in *Escherichia coli* via the LacR/O, the TetR/O and AraC/I1-I2 regulatory elements. Nucleic Acids Res. 25, 1203–1210.

Malla, S., Koffas, M.A., Kazlauskas, R.J., Kim, B.G., 2012. Production of 7-O-methyl aromadendrin, a medicinally valuable flavonoid, in *Escherichia coli*. Appl. Environ. Microbiol. 78, 684–694.

Mellin, J.R., Tiensuu, T., Becavin, C., Gouin, E., Johansson, J., Cossart, P., 2013. A riboswitch-regulated antisense RNA in *Listeria monocytogenes*. Proc. Natl. Acad. Sci. USA 110, 13132–13137.

Minkler, P.E., Kerner, J., Kasumov, T., Parland, W., Hoppel, C.L., 2006. Quantification of malonyl-coenzyme A in tissue specimens by high-performance liquid chromatography/mass spectrometry. Anal. Biochem. 352, 24–32.

Na, D., Yoo, S.M., Chung, H., Park, H., Park, J.H., Lee, S.Y., 2013. Metabolic engineering of *Escherichia coli* using synthetic small regulatory RNAs. Nat. Biotechnol. 31, 170–174.

Nakashima, N., Tamura, T., 2009. Conditional gene silencing of multiple genes with antisense RNAs and generation of a mutator strain of *Escherichia coli*. Nucleic Acids Res. 37, e103.

Nakashima, N., Tamura, T., Good, L., 2006. Paired termini stabilize antisense RNAs and enhance conditional gene silencing in *Escherichia coli*. Nucleic Acids Res. 34, e138.

Olano, C., Mendez, C., Salas, J.A., 2011. Molecular insights on the biosynthesis of antitumour compounds by actinomycetes. Microb. Biotechnol. 4, 144–164.

Onorato, J.M., Chen, L., Shipkova, P., Ma, Z., Azzara, A.V., Devenny, J.J., Liang, N., Haque, T.S., Cheng, D., 2010. Liquid-liquid extraction coupled with LC/MS/MS for monitoring of malonyl-CoA in rat brain tissue. Anal. Bioanal. Chem. 397, 3137–3142.

Patnaik, R., Roof, W.D., Young, R.F., Liao, J.C., 1992. Stimulation of glucose catabolism in *Escherichia coli* by a potential futile cycle. J. Biotechnol. 174, 7527–7532.

Price, A.C., Choi, K.H., Heath, R.J., Li, Z., White, S.W., Rock, C.O., 2001. Inhibition of beta-ketoacyl-acyl carrier protein synthases by thiolactomycin and cerulenin. Structure and mechanism. J. Biol. Chem. 276, 6551–6559.

Rapp, M., Drew, D., Daley, D.O., Nilsson, J., Carvalho, T., Melen, K., De Gier, J.W., Von Heijne, G., 2004. Experimentally based topology models for *E. coli* inner membrane proteins. Protein Sci. 13, 937–945.

Rathnasingh, C., Raj, S.M., Lee, Y., Catherine, C., Ashok, S., Park, S., 2012. Production of 3-hydroxypropionic acid via malonyl-CoA pathway using recombinant *Escherichia coli* strains. J. Biotechnol. 157, 633–640.

Santos, C.N., Koffas, M., Stephanopoulos, G., 2011. Optimization of a heterologous pathway for the production of flavonoids from glucose. Metab. Eng. 13, 392–400.

Scalcinati, G., Knuf, C., Partow, S., Chen, Y., Maury, J., Schalk, M., Daviet, L., Nielsen, J., Siewers, V., 2012. Dynamic control of gene expression in *Saccharomyces cerevisiae* engineered for the production of plant sesquitepene alpha-santalene in a fed-batch mode. Metab. Eng. 14, 91–103.

Sharma, V., Sakai, Y., Smythe, K.A., Yokobayashi, Y., 2013. Knockdown of recA gene expression by artificial small RNAs in *Escherichia coli*. Biochem. Biophys. Res. Commun. 430, 256–259.

Shen, C.R., Liao, J.C., 2008. Metabolic engineering of *Escherichia coli* for 1-butanol and 1-propanol production via the keto-acid pathways. Metab. Eng. 10, 312–320.

Shi, S., Chen, Y., Siewers, V., Nielsen, J., 2014. Improving production of malonyl coenzyme A-derived metabolites by abolishing Snf1-dependent regulation of Acc1. MBio 5, e01130–14.

Solomon, K.V., Sanders, T.M., Prather, K.L., 2012. A dynamic metabolite valve for the control of central carbon metabolism. Metab. Eng. 14, 661–671.

Storz, G., Vogel, J., Wassarman, K.M., 2011. Regulation by small RNAs in bacteria: expanding frontiers. Mol. Cell 43, 880–891.

Thomason, M.K., Storz, G., 2010. Bacterial antisense RNAs: how many are there, and what are they doing? Annu. Rev. Genet. 44 (44), 167–188.

Tummala, S.B., Welker, N.E., Papoutsakis, E.T., 2003. Design of antisense RNA constructs for downregulation of the acetone formation pathway of *Clostridium acetobutylicum*. J. Bacteriol. 185, 1923–1934.

Wang, B., Kuramitsu, H.K., 2005. Inducible antisense RNA expression in the characterization of gene functions in *Streptococcus* mutans. Infect. Immun. 73, 3568–3576.

Wu, J.J., Yu, O., Du, G.C., Zhou, J.W., Chen, J., 2014. Fine-tuning of the fatty acid pathway by synthetic antisense RNA for enhanced (2S)-naringenin production from L-Tyrosine in *Escherichia coli*. Appl. Environ. Microbiol. 80, 7283–7292.

Xu, P., Gu, Q., Wang, W., Wong, L., Bower, A.G., Collins, C.H., Koffas, M.A., 2013. Modular optimization of multi-gene pathways for fatty acids production in *E. coli*. Nat. Commun. 4, 1409.

Xu, P., Li, L., Zhang, F., Stephanopoulos, G., Koffas, M., 2014a. Improving fatty acids production by engineering dynamic pathway regulation and metabolic control. Proc. Natl. Acad. Sci. USA 111, 11299–11304.

Xu, P., Wang, W., Li, L., Bhan, N., Zhang, F., Koffas, M.A., 2014b. Design and kinetic analysis of a hybrid promoter-regulator system for malonyl-CoA sensing in *Escherichia coli*. ACS Chem. Biol. 9, 451–458.

Yan, Y., Chemler, J., Huang, L., Martens, S., Koffas, M.A., 2005a. Metabolic engineering of anthocyanin biosynthesis in *Escherichia coli*. Appl. Environ. Microbiol. 71, 3617–3623.

Yan, Y., Li, Z., Koffas, M.A., 2008. High-yield anthocyanin biosynthesis in engineered *Escherichia coli*. Biotechnol. Bioeng. 100, 126–140.

Yan, Y.J., Kohli, A., Koffas, M.A.G., 2005b. Biosynthesis of natural flavanones in *Saccharomyces cerevisiae*. Appl. Environ. Microbiol. 71, 5610–5613.

Yoo, S.M., Na, D., Lee, S.Y., 2013. Design and use of synthetic regulatory small RNAs to control gene expression in *Escherichia coli*. Nature Protocols 8, 1694–1707.

Zha, W., Rubin-Pitel, S.B., Shao, Z., Zhao, H., 2009. Improving cellular malonyl-CoA level in *Escherichia coli* via metabolic engineering. Metab. Eng. 11, 192–198.